EC
Journals.ASM.org

Mutations on the N-Terminal Edge of the DELSEED Loop in either the α or β Subunit of the Mitochondrial F_1-ATPase Enhance ATP Hydrolysis in the Absence of the Central γ Rotor

Thuy La,[a] George Desmond Clark-Walker,[b,c] Xiaowen Wang,[a] Stephan Wilkens,[a] Xin Jie Chen[a]

Department of Biochemistry and Molecular Biology, State University of New York Upstate Medical University, Syracuse, New York, USA[a]; Research School of Chemistry[b] and Research School of Biology,[c] The Australian National University, Canberra, Australia

F_1-ATPase is a rotary molecular machine with a subunit stoichiometry of $\alpha_3\beta_3\gamma_1\delta_1\epsilon_1$. It has a robust ATP-hydrolyzing activity due to effective cooperativity between the three catalytic sites. It is believed that the central γ rotor dictates the sequential conformational changes to the catalytic sites in the $\alpha_3\beta_3$ core to achieve cooperativity. However, recent studies of the thermophilic *Bacillus* PS3 F_1-ATPase have suggested that the $\alpha_3\beta_3$ core can intrinsically undergo unidirectional cooperative catalysis (T. Uchihashi et al., Science 333:755-758, 2011). The mechanism of this γ-independent ATP-hydrolyzing mode is unclear. Here, a unique genetic screen allowed us to identify specific mutations in the α and β subunits that stimulate ATP hydrolysis by the mitochondrial F_1-ATPase in the absence of γ. We found that the F446I mutation in the α subunit and G419D mutation in the β subunit suppress cell death by the loss of mitochondrial DNA (ρ^o) in a *Kluyveromyces lactis* mutant lacking γ. *In organello* ATPase assays showed that the mutant but not the wild-type γ-less F_1 complexes retained 21.7 to 44.6% of the native F_1-ATPase activity. The γ-less F_1 subcomplex was assembled but was structurally and functionally labile *in vitro*. Phe446 in the α subunit and Gly419 in the β subunit are located on the N-terminal edge of the DELSEED loops in both subunits. Mutations in these two sites likely enhance the transmission of catalytically required conformational changes to an adjacent α or β subunit, thereby allowing robust ATP hydrolysis and cell survival under ρ^o conditions. This work may help our understanding of the structural elements required for ATP hydrolysis by the $\alpha_3\beta_3$ subcomplex.

Mitochondria are the powerhouses of the cell that synthesize the majority of ATP required to support cellular activities under aerobic conditions. Although mitochondria are known to be essential for cell viability and mitochondrial stress induces cell death, the key mitochondrial factors that determine cell viability under specific stress conditions are not well established. One of the classic inducers of mitochondrial stress is the loss of mitochondrial DNA (mtDNA). In the budding yeast *Saccharomyces cerevisiae* and some other closely related species, petite mutants with extensively deleted mtDNA (ρ^-) or a complete loss of mtDNA (ρ^o) are viable (1–5). However, most yeast species, known as petite negative, do not survive the loss of mtDNA on exposure to mutagens. The loss of cell viability is not caused by a bioenergetic crisis. For instance, a petite-negative yeast such as *Kluyveromyces lactis* can survive on glucose medium after disruption of the cytochrome *c* gene but cannot survive the elimination of mtDNA (6). *K. lactis* is therefore capable of synthesizing ATP to support cell growth via fermentative glycolysis, so lethality from ρ^o (ρ^o lethality) is caused by factors other than ATP depletion.

Our previous studies have shown that specific nuclear mutations can suppress lethality from ρ^o in *K. lactis*. These mutations, referred to as *mgi* (for *mitochondrial genome integrity*), occur in the α, β, and γ subunits of the mitochondrial F_oF_1-ATP synthase (7–9). The ATP synthase is a rotary molecular machine that synthesizes ATP from ADP and inorganic phosphate by using the proton gradient generated by the electron transport chain (10, 11). It consists of the transmembrane F_o domain and the F_1-ATPase extending into the mitochondrial matrix. The catalytic F_1 contains nine polypeptides with the stoichiometry of $\alpha_3\beta_3\gamma\delta\epsilon$. The readmission of protons from the intermembrane space to the mitochondrial matrix through F_o drives the rotation of γ within

the $\alpha_3\beta_3$ hexameric ring, which induces the conformational changes necessary for the synthesis of ATP (12, 13). The F_1-ATPase can be dissociated from the membrane-embedded F_o. In free F_1, γ rotates in the reverse direction, allowing hydrolysis but not synthesis of ATP. It has been believed that the rotating γ plays a key role in coordinating sequential conformational changes in the three catalytic sites, which confers a highly cooperative and robust mechanism for ATP hydrolysis.

In yeast cells with ρ^o (ρ^o cells), F_o is eliminated because of the loss of the mtDNA-encoded Atp6, -8, and -9 subunits. The gain-of-function *mgi* mutations confer on the remaining F_1 domain a novel property that permits cell survival. A widely accepted model is that the mutant F_1 remains active in hydrolyzing ATP^{-4} that is glycolytically generated in the cytosol before being imported into the matrix. The mutant F_1, but not the wild type F_1, hydrolyzes ATP^{-4} to ADP^{-3}, which is subsequently exported to the cytosol. This reversed exchange of cytosolic ATP^{-4} against the matrix ADP^{-3} via the adenine nucleotide translocase is electrogenic, which allows the mitochondria to maintain the minimal membrane potential ($\Delta\psi_m$) required for mitochondrial biogenesis (14–16). A large genetic screen has identified 35 *mgi* alleles in *K. lactis* (9). A similar mutation in the γ subunit of F_1-ATPase that suppresses the slow-growth phenotype of ρ^o cells in the *yme1* back-

ground has also been reported in *Saccharomyces cerevisiae* (17). Interestingly, all the mutable residues are mapped to two specific regions, with one suggested to be a molecular bearing for the rotation of γ within the α₃β₃ hexamer and the other being proximal to the membrane close to the conserved DELSEED loop in β and its equivalent in α. At these two particular locations, all the mutated amino acids are situated on the interface between the α, β, and γ subunits. This suggests that the suppressor mutations affect subunit-subunit interactions. The mutant F₁ appears to have a lower K_m for ATP than the wild-type enzyme (18). The altered kinetic property may allow the mutant complexes to continue to hydrolyze ATP in ρ° cells in which the matrix ATP concentration might be low. By introducing the *mgi* mutations into the *S. cerevisiae* F₁ complex, the Mueller group found that the mutant ATP synthase is uncoupled (19). Four mutant F₁ complexes were crystallized, and their structures were analyzed (20). Interestingly, the *mgi* mutations were found either to affect substrate (phosphate) binding or to reduce the steric hindrance imposed by the β subunit when γ rotates in the α₃β₃ core.

In an attempt to identify nuclear mutations that potentially suppress ρ° lethality in the absence of ATP hydrolysis by F₁-ATPase, we screened suppressor mutations in a strain lacking the γ subunit. Surprisingly, this unique genetic screen yielded two mutations that are again mapped to the α and β subunits. These mutations apparently confer a robust ATP-hydrolyzing activity in the absence of γ. This finding provides strong *in vivo* evidence supporting the newly emerging paradigm that robust catalysis can take place in the α₃β₃ core.

MATERIALS AND METHODS

Media and strains. Yeast cells were grown in complete glucose medium containing 1% yeast extract, 2% Bacto peptone, and 2% glucose (YPD) or in minimum medium containing 6.7 g/liter Bacto yeast nitrogen base without amino acids (Difco) and 2% glucose. Nutrients essential for auxotrophic strains were added at 25 μg/ml for bases and 50 μg/ml for amino acids. Complete glycerol-ethanol medium and glycerol medium contained 1% yeast extract, 2% Bacto peptone, and 2% glycerol with or without 2% ethanol (YPGE and YPG, respectively). Where indicated, ethidium bromide (EB) was added at a concentration of 16 μg/ml. G418 medium was YPD plus G418 at 200 μg/ml. For sporulation of *K. lactis*, ME medium contained 5% malt extract and 2% Bacto agar.

The yeast strains used in this study are listed in Table 1. Standard procedures were used for the construction of *K. lactis* strains. Transformation of *K. lactis* was performed by the lithium acetate-dimethyl sulfoxide method as previously described in detail (21). For selection of G418-resistant transformants, transformed cells were grown at room temperature overnight before being plated on G418 medium. Disruption of the chromosomal genes was achieved by a one-step gene replacement procedure. To construct the *atp3Δ::URA3* allele, pBS-MGI5, a pBluescript-based plasmid containing the entire *ATP3* gene, was digested with ClaI. The 0.75-kb ClaI fragment comprising the N-terminal two-thirds of the *ATP3* sequences and part of the promoter region was deleted and replaced by the 1.1-kb *URA3* gene (see Fig. 1B). The resulting plasmid, pMGI5Δ::URA3, was digested with EcoRI to release the 1.5-kb *atp3Δ::URA3* cassette, which was subsequently used for disruption of *ATP3* in various strains. The *atp3::kan* cassette was isolated from plasmid pMGI5::kan/3 in which *ATP3* was disrupted by insertion of *kan* at codon 161.

The plasmids pCXJ4-MGI2 and pCXJ4-MGI1/7 are based on the *K. lactis* integrative vector pCXJ4 (X. J. Chen, unpublished data) and contain *K. lactis ATP1* (*KlATP1*) and *K. lactis ATP2* (*KlATP2*), respectively. The two plasmids were linearized with ClaI, which cuts within the *K. lactis LEU2* gene, before being integrated onto the chromosome by selecting for

TABLE 1 Genotypes and sources of *K. lactis* strains used in this study

Strain	Relevant genotype	Source or reference
CK56-16C	*MATα ade1 lysA1 uraA1*	7
CK98-8A	*MATα ade1 metA1 uraA1 atp2-3*	Chen lab
CK141-4A	*MATa lysA1 uraA1 atp1-2*	Chen lab
CK196/1	*MATa adeT-600 uraA1 atp1Δ::URA3*	7
CK204	*MATa adeT-600 uraA1 atp3Δ::URA3*	7
CK204/EB2	*MATa adeT-600 uraA1 atp3::URA3 atp2-12*	This study
CK204/EB3	*MATa adeT-600 uraA1 atp3::URA3 atp2-12*	This study
CK204/EB4	*MATa adeT-600 uraA1 atp3::URA3 atp1-7*	This study
CK204/EB8	*MATa adeT-600 uraA1 atp3::URA3 atp2-12*	This study
CK292	Same as CW13-4C but *LEU2::pCXJ4-MGI/7*	This study
CK295	Same as CW15-6C but *LEU2::pCXJ4-MGI2*	This study
CK306	*MATa ade1 uraA1 atp3Δ::URA3*	This study
CK307	*MATa lysA1 uraA1 atp2-12 atp3Δ::URA3*	This study
CK308	*MATa adeT-600 uraA1 atp1-7 atp3Δ::URA3*	This study
CK312	CW14-4D × CK98-8A	This study
CK314-2B	*MATα Ade⁻ uraA1 atp2-12 atp1-7*	This study
CK316-2C	*MATa adeT-600 uraA1 leu2 atp2::URA3 atp3::URA3*	Chen lab
CK325	CW15-2A × CK141-4A	This study
CK326	*MATα Ade⁻ uraA1 atp2-12 atp1-7 atp3Δ::URA3*	This study
CK333	*MATα ade1 adeT-600 uraA1 leu2 atp1Δ::kan atp3::URA3*	Chen lab
CK391/18	*MATα ade1 uraA1 leu2 lysA1 atp2-12*	This study
CK392/7	*MATα ade1 uraA1 leu2 atp1-7*	This study
CK400	*MATα ade1 uraA1 leu2 lysA1 atp2-12 atp3::kan*	This study
CK401/1	*MATα ade1 uraA1 leu2 atp1-7 atp3::kan*	This study
CK405	*MATα ade1 uraA1 leu2 lysA1 atp2-12 atp3::kan atpδ::URA3*	This study
CK406	*MATα ade1 uraA1 leu2 lysA1 atp2-12 atp3::kan atpε::LEU2*	This study
CK408	*MATα ade1 uraA1 leu2 atp1-7 atp3::kan atpδ::URA3*	This study
CK409	*MATα ade1 uraA1 leu2 atp1-7 atp3::kan atpε::URA3*	This study
CK410/6	*MATα ade1 uraA1 leu2 atp2-12 atp3::kan atpδ::URA3 atpε::LEU2*	This study
CK412/1	*MATα ade1 uraA1 leu2 atp1-7 atp3::kan atpδ::URA3 atpε::LEU2*	This study
CW13	CK56-16C × CK204/EB2	This study
CW13-4C	*MATa lysA1 uraA1 atp2-12*	This study
CW14	CK56-16C × CK204/EB3	This study
CW14-1A	*MATα ade1 uraA1 atp2-12*	This study
CW14-4D	*MATa lysA1 uraA1 atp2-12*	This study
CW15	CK56-16C × CK204/EB4	This study
CW15-2A	*MATα ade1 uraA1 atp1-7*	This study
CW15-6C	*MATa adeT-600 uraA1 atp1-7*	This study
CW16	CK56-16C × CK204/EB8	This study
CW16-7C	*MATa adeT-600 lysA1 uraA1 atp2-12*	This study
PM6-7A	*MATa adeT-600 uraA1*	55
TL1/1	*MATα ade1 adeT-600 uraA1 leu2 atp1Δ::kan atp3::URA3 leu2::pCXJ4-MGI2 His₆/7/ClaI*	This study
TL2/2	*MATα ade1 adeT-600 uraA1 leu2 atp1Δ::kan atp3::URA3 leu2::pCXJ4-sym2.1 (atp1-7)His/1/ClaI*	This study
TL3/4	*MATα ade1 adeT-600 uraA1 leu2 atp1Δ::kan atp3::URA3 leu2::pCXJ4-MGI2/ClaI*	This study

Leu⁺ transformants. pUK-KlMGI2/HP and pCXJ22-KlATP2 are multicopy plasmids for *K. lactis* containing *KlATP1* and *KlATP2*, respectively.

CK392/7 (*atp1-7*) and CK391/18 (*atp2-12*) are random spores derived from CW15-2A and CW14-1A, respectively. Replacement of *ATP3* by *atp3::kan* in the two strains yielded CK401 and CK400, respectively. Successive disruption of *ATPδ* and *ATPε* in CK401/1 and CK400 by the *atpδ::URA3* and *atpε::LEU2* cassettes produced the triple-disrupted strains CK412/1 and CK410/6, respectively.

For His₆ tagging of *ATP1* in the *atp3Δ* background, we constructed the plasmid pCXJ4-sym2.1(atp1-7)His, in which the allele with the F-to-I change at position 446 encoded by *atp1* (*atp1^F446I*) was tagged with His₆ on the C terminus. The plasmid was linearized with ClaI within the *LEU2* gene and integrated into the *leu2* locus of CK333 (αΔ γΔ) by selecting for

Leu⁺ transformants. This generated strain TL2/2. Correct integration of the plasmid was confirmed by PCR-based genotyping.

Purification of F₁-ATPase. Mitochondria were isolated as described by Boldogh and Pon (22). Yeast cells were grown in high-glucose minimum medium, washed with Tris-SO_4-dithiothreitol (DTT) buffer, treated with 5 mg zymolyase per gram of yeast to create spheroplasts, and then broken with a 40-ml Dounce homogenizer. Mitochondria were collected by differential centrifugation.

His₆-tagged F₁-ATPases were purified by Ni column chromatography as described by Mueller et al., with modifications (23). Briefly, crude mitochondria were resuspended in sonication buffer (0.25 M sucrose, 20 mM HEPES-KOH, pH 7.4, 5 mM ε-amino caproic acid, 1 mM EDTA, 1 mM phenylmethylsulfonyl fluoride [PMSF]) at a ratio of 1:2, by volume. Sonication was performed on ice 4 times for 1 min each time, with 1-min intervals used between each sonication. The inverted mitochondrial solution was centrifuged at 6,400 rpm at 4°C for 5 to 10 min. The supernatant was then collected and added to a Ni-nitrilotriacetic acid (NTA) slurry containing 50% beads and 50% buffer A (0.05 M NaCl, 0.25 M sucrose, 20 mM HEPES-KOH, pH 7.4, 5 mM ε-amino caproic acid, and 1 mM PMSF plus 3% buffer B [0.1 M imidazole, 0.05 M NaCl, 0.25 M sucrose, 20 mM HEPES-KOH, pH 7.4, 5 mM ε-amino caproic acid, 1 mM PMSF]). The ratio of sample solution to Ni-NTA slurry was 60:1, by volume. The solution was gently rocked at 4°C for 4 to 5 h before it was centrifuged at 2,000 × *g* for 1 min at 4°C. The beads were washed twice with buffer A containing 3% buffer B, and F₁-ATPases were eluted from the Ni beads 4 times using 0.3 ml buffer B per elution. The wild-type F₁-ATPase was also purified as described by Mueller and coworkers before being analyzed by size exclusion chromatography (23).

BN-PAGE. Blue native (BN)-PAGE was performed using a Life Technologies (Carlsbad, California) native PAGE Novex bis-Tris gel system as recommended by the manufacturer. The nickel column pull-down products were separated on a 3 to 12% polyacrylamide gradient gel at 4°C. The final concentration of the native PAGE G-250 sample additive used was 0.5%. No other detergent was needed. Western blotting was performed using antibodies specific for the α or β subunit of the yeast F₁-ATPases. Signals were detected using an enhanced chemiluminescence detection method (Roche and Thermo Scientific). For BN-PAGE of the mitochondrial lysate, the final concentration of digitonin used to solubilize mitochondria was 2%, and the concentration of native PAGE G-250 sample additive used was 1/3 of the digitonin concentration.

Size exclusion chromatography. The His₆-tagged γ-less F₁-ATPases from strains TL1/1 and TL2/2 were prepared as described above. The sonication buffer used to resuspend crude mitochondria contained no EDTA to prevent the stripping of Ni from the column. Sonication was performed on ice 4 times at half cycle for 30 s each time, with 30-s intervals used between each sonication. The solution containing inverted mitochondria was centrifuged at 13,000 rpm at 4°C for 30 min. Clear supernatant was collected and incubated with 1 ml of Ni-NTA slurry containing 50% beads and 50% buffer A for 30 to 60 min at 4°C. The mixture was then passed through a vertical column, washed 3 times with buffer A, and eluted 6 times with 500 μl buffer B containing 200 mM instead of 100 mM imidazole. The proteins were concentrated and analyzed by size exclusion chromatography on a calibrated Superdex 200 10/30 column equilibrated with 50 mM NaCl, 20 mM HEPES, pH 7.4, 5 mM ε-amino caproic acid, 1 mM DTT, 1 mM ATP, 250 mM sucrose, and 1 mM EDTA. Peak fractions were analyzed by SDS-PAGE and Western blotting.

ATPase activity assays. ATPase activity was measured as described by Taussky and Schorr (24), with modifications. Five to 10 μl (approximately 0.1 to 0.2 mg) of mitochondria was added to 3 ml of 10 mM Tris-HCl (pH 8.2), 5 mM ATP, 2 mM $MgCl_2$, and 200 mM KCl with or without oligomycin at 10 μg/ml. The reaction mixtures were incubated at 30°C for 10 min before quenching with 10% SDS. All samples were gently vortexed to avoid inactivation of enzymes. ATPase activity is expressed as μmol ATP hydrolyzed/min/mg protein.
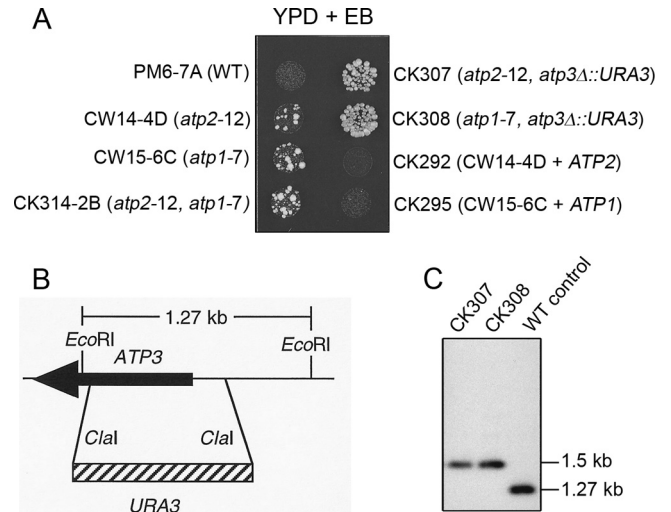

FIG 1 Suppression of ρ° lethality by the *atp1-7* and *atp2-12* alleles after the deletion of *ATP3* encoding the γ subunit of F₁-ATPase. (A) Growth phenotype of *K. lactis* cells on EB medium, which eliminates mtDNA. Cells were grown in YPD medium, diluted to an equal density in water, and spotted on YPD medium supplemented with EB. The cells were then incubated at 28°C for 7 days before being photographed. (B) Schematic showing the strategy for the disruption of the *ATP3* gene encoding the γ subunit of F₁-ATPase. (C) Southern blot analysis showing the disruption of *ATP3* in CK307 (*atp2-12 atp3Δ::URA3*) and CK308 (*atp1-7 atp3Δ::URA3*). WT, wild type.

RESULTS

Isolation of the *atp1-7* and *atp2-12* mutations. In *S. cerevisiae*, the γ subunit is required for the assembly of F₁-ATPase (25). In an attempt to isolate mutations that suppress ρ° lethality from *K. lactis* in the absence a functionally active F₁, we screened for EB-resistant (EBr) colonies from CK204 disrupted in the *ATP3* gene encoding the γ protein. We have previously reported that CK204 is petite negative and unable to form colonies on EB, which specifically eliminates mtDNA (7) (see below). CK204 was thus plated on EB medium and incubated for 7 days at 28°C. Fast-growing EBr papillae were scored. The EBr clones all lacked mtDNA, as confirmed by Southern blot analysis of total DNA prepared from the mutant cells by using total *K. lactis* mtDNA as a probe (data not illustrated).

Genetic analysis was performed to identify putative suppressor mutations that permitted the survival of the γΔ and ρ° cells. The four EB-resistant isolates CK204/EB2, CK204/EB3, CK204/EB4, and CK204/EB8 were crossed to the wild-type strain CK56-16C. The resulting diploids, CW13, CW14, CW15, and CW16, respectively, were sporulated, and 12 asci were dissected from each strain. Phenotypic examination of the segregants indicated that respiratory deficiency, as judged from failure to grow on nonfermentable YPGE medium, segregated 2⁺:2⁻ in all tetrads. The respiration-deficient phenotype cosegregated with Ura⁺, marking the disruption of *ATP3* in the parental strain CK204. When segregants were spotted onto EB plates that were incubated for 5 days at 28°C, two interesting observations were made. First, approximately 50% of respiration-deficient segregants were resistant to EB, suggesting the presence of a mutation that is capable of suppressing ρ° lethality in the absence of the γ subunit, as exemplified by CK307 and CK308 (Fig. 1A). Second, about 50% of the respiration-competent segregants formed papillae on EB plates, as ex-
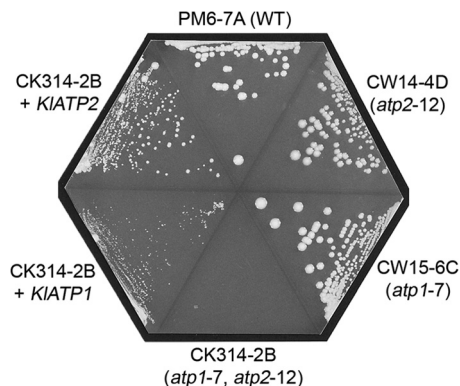
FIG 2 Respiratory growth phenotype of *K. lactis atp1-7* and *atp2-12* mutants. Cells were streaked on the nonfermentable YPG (glycerol) medium and incubated at 28°C for 4 days, before being photographed. The double mutant CK314-2B (*atp1-7 atp2-12*) was transformed with the plasmids pUK-KlMGI2/HP and pCXJ22-KlATP2 expressing the wild-type *ATP1* and *ATP2* genes, respectively. A representative transformant was streaked on the plate and tested for respiratory growth.

emplified by CW14-4D and CW15-6C. However, these strains did not have the same level of EB resistance as CK307 and CK308. When these apparently weak mutations were combined with disruption of *ATP3*, strains (e.g., CK307 and CK308; Fig. 1A) that had high levels of resistance to EB were formed. As described below, we subsequently found that the suppressor mutations in CK204/EB4 occur in *ATP1*, encoding the α subunit of F_1-ATPase. Consequently, the mutation was designated *atp1-7*. As the mutations in strains CK204/EB2, CK204/EB3, and CK204/EB8 have the same change in the *ATP2* gene, encoding the β subunit of F_1-ATPase, this allele was referred to as *atp2-12*.

Both the *atp1-7* and *atp2-12* mutants were respiration competent in the presence of γ, and no significant difference in the growth rate on glycerol plates compared with that of wild-type strain PM6-7A was noticeable (Fig. 2). These cells did not form spontaneous respiration-deficient mutants on YPD medium (data not shown). As shown in Fig. 1A, EB^r colonies arose at a high frequency for strains CW15-6C (*atp1-7*) and CW14-4D (*atp2-12*). Quantitative estimation revealed that CW15-6C and CW14-4D formed EB^r colonies at frequencies of 5.6×10^{-2} and 2.6×10^{-2}, respectively, which are significantly higher than the frequency of 1.1×10^{-4} found in *K. lactis* wild-type strain PM6-7A. EB^r papillae were also observed in the *atp1-7 atp2-12* double mutant CK314-2B at a frequency of 8.0×10^{-2}, which was higher than the frequencies in the *atp1-7* and *atp2-12* single mutants (Fig. 1A). These observations support the idea that the *atp1-7* and *atp2-12* mutants have poor survival after the elimination of mtDNA by EB. The disruption of *ATP3* from these cells improved cell viability (see below).

As the *atp3::URA3* allele in CK204 used for the isolation of the *atp1-7* and *atp2-12* alleles was constructed by a simple insertion of the *URA3* marker at codon 161 (7), it might be possible that a truncated version of the γ protein with the N-terminal sequence is produced and incorporated into the F_1 complex. To address this issue, we constructed the *atp3Δ::URA3* allele in which the promoter sequence and majority of the coding region of *ATP3* were replaced by *URA3* (Fig. 1B). This cassette was introduced into CW15-6C (*atp1-7*) and CW14-4D (*atp2-12*) to replace the wild-

type *ATP3*. The correct replacement was confirmed by Southern blot analysis of genomic DNA. As shown in Fig. 1C, the strains with the *ATP3* deletion, CK308 and CK307, had a band of 1.5 kb that hybridized to the 1.5-kb EcoRI-EcoRI *ATP3* probe instead of a band of 1.27 kb in a wild-type control strain, which is expected for the correct replacement of the chromosomal *ATP3* by *atp3Δ::URA3*. Because both CK308 and CK307 grew on EB medium (Fig. 1A), the data further confirm that the activity of the *atp1-7* or *atp2-12* allele in suppressing ρ° lethality is enhanced by the complete lack of the γ protein. When *ATP3* was disrupted in CK314-2B (*atp1-7 atp2-12*), the resulting strain, CK326, also displayed an EB^r (or petite-positive) phenotype (data not illustrated).

The mutations occur in the *ATP1* and *ATP2* genes encoding the α and β subunits of F_1-ATPase. To identify the mutations that suppress ρ° lethality in the γ-less strains, we first considered whether the *ATP1* and *ATP2* genes, encoding the α and β subunits of F_1-ATPase, respectively, might have been mutated. Indeed, we found that the mutations occurred in the two genes. When plasmid pCXJ4-MGI2, carrying the *ATP1* gene, was integrated into the *LEU2* locus of CW15-6C (*atp1-7*), the formation of papillae on EB medium was suppressed in the resulting strain, CK295 (Fig. 1A), whereas transformation by pCXJ4-MGI1/7, bearing *ATP2*, did not suppress the EB^r papilla phenotype (data not illustrated). The results suggest that the mutation in CW15-6C might occur in *ATP1*. This allele, initially derived from CK204/EB4, was thus tentatively designated *atp1-7*. Likewise, when pCXJ4-MGI1/7, bearing the *ATP2* gene, was integrated into CW13-4C, CW14-4D, and CW16-7C, derived from CK204/EB2, CK204/EB3, and CK204/EB8, respectively, the resulting strains, CK292 (Fig. 1A), CK291, and CK293, respectively (data not illustrated), did not show the EB^r papilla phenotype. Introduction of pCXJ4-MGI2 (*ATP1*) did not suppress the formation of EB^r papillae in the three strains. As the isolates carry the same lesion in *ATP2* (see below), the mutation was designated *atp2-12*.

Further experiments were performed to confirm that the γ-independent ρ° lethality suppressor mutations occur in *ATP1* and *ATP2*. First, we found that, in contrast to the *atp1-7* and *atp2-12* single mutants, which are respiration competent, the double mutant CK314-2B failed to grow on glycerol medium (Fig. 2). However, transformation of CK314-2B with the plasmids pUK-KlMGI2/HP and pCXJ22-KlATP2, carrying the *KlATP1* and *KlATP2* genes, respectively, could partially restore growth on YPG (Fig. 2). The complementation of respiratory deficiency by the two genes suggests that the two mutations in CK314-2B may have occurred in *ATP1* and *ATP2*.

Second, we crossed CW15-2A (*atp1-7*) to CK141-4A (*atp1-2*) and CW14-4D (*atp2-12*) to CK98-8A (*atp2-3*). *K. lactis* cells carrying the *atp1-2* or *atp2-3* allele are viable with ρ° and resistant to EB (7, 8). The resulting diploid strains, CK325 and CK312, respectively, were sporulated, and 12 tetrads were dissected from each strain. When the segregants were examined for their response to EB, it was found that in all tetrads, two spores were EB^r, while the other two spores formed EB^r papillae on EB plates (data not illustrated). These data indicate that the mutation in CW15-2A is allelic to *ATP1*, and the one in CW14-4D is allelic to *ATP2*.

Identification of the mutations in the *atp1-7* and *atp2-12* alleles. The *ATP1* gene from CK204/EB4 (*atp1-7*) was amplified by PCR, and the complete coding region was sequenced. Compared with the sequences in the wild-type allele in the parental strain
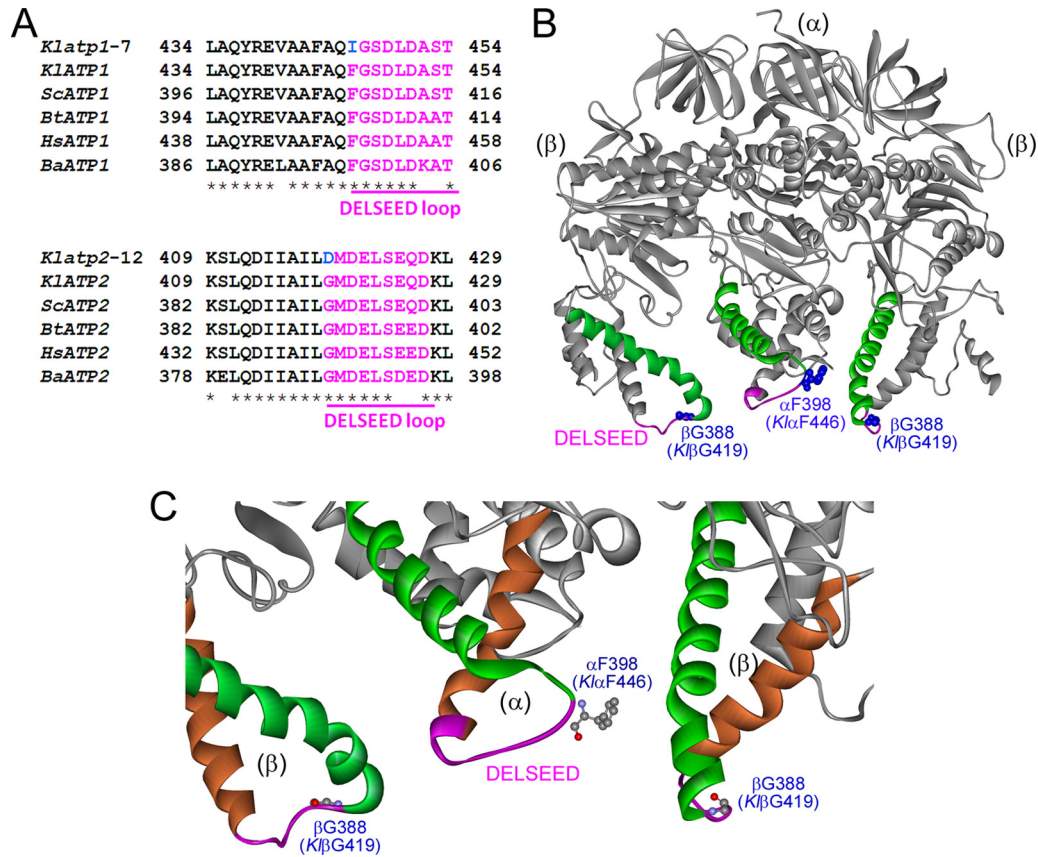
FIG 3 The *atp1-7* and *atp2-12* mutations occur on the N-terminal edge of the DELSEED loops in the α and β subunits of F₁-ATPase. (A) Comparison of amino acid sequences from various organisms of the DELSEED loop regions where the *Klatp1-7* and *Klatp2-12* mutations occur. The DELSEED loop sequences are highlighted in pink. αPhe446 and βGly419 are converted to Ile and Asp (green), respectively, in the *Klatp1-7* and *Klatp2-12* mutants, respectively. *Kl*, *K. lactis*; *Sc*, *S. cerevisiae*; *Bt*, *Bos taurus*; Hs, *Homo sapiens*; *Ba*, thermophilic *Bacillus*. (B) Crystal structure of the α₃β₃ core of F₁-ATPase from thermophilic *Bacillus* PS3 (Protein Data Bank accession number 1SKY). For clarity, only half of the symmetric α₃β₃ core is shown. The DELSEED loops are highlighted in pink, and the N-terminal α helix preceding the DELSEED loops is shown in green. The amino acids αF398 and βG388 correspond to αF446 and βG419, respectively, which are mutated in the *K. lactis atp1-7* and *atp2-12* mutants, respectively. (C) Close-up view at the DELSEED loops in the α and β subunits, which may interact with each other in the γ-less enzyme.

PM6-7A used for the isolation of *atp1-7*, two mutations were found. The codons 435 and 446 were changed from GCC and ACC to ACC and ATC, respectively. These changes convert Ala435 into Thr and Phe446 into Ile. To delineate which mutation is responsible for ρ° lethality suppression in the γΔ background, alleles with the single mutations A435T and F446I in the α subunit (αA435T and αF446I, respectively) were generated by site-directed *in vitro* mutagenesis. The mutant alleles were cloned into the *K. lactis* vector pCXJ4 and integrated into the *LEU2* locus of CK333 (αΔ γΔ) by selecting for Leu⁺ transformants. Following the test on EB plates, it was found that only the αF446I allele and not the αA435T allele conferred the EBʳ phenotype. We thus concluded that in the initial *atp1-7* mutant, the αF446I mutation is responsible for the suppression of ρ° lethality in γΔ cells. The amino acid αPhe446 is highly conserved in the α subunit of F₁-ATPase in organisms from bacteria to humans (Fig. 3A).

Likewise, we amplified the *ATP2* gene from the EBʳ isolates CK204/EB2, CK204/EB3, and CK204/EB8. The entire coding region of the gene was sequenced and compared with that of the wild type. A single mutation that changed codon 419 from GGT to GAT, which converted Gly419 to Asp, was found in the three

isolates. βGly419 is also highly conserved during evolution (Fig. 3A).

The δ and ε subunits are dispensable for the suppressor activity of the *atp1-7* and *atp2-12* alleles. To assess whether the two other small subunits of F₁, δ and ε, play a role in the phenotypic manifestation of the *atp1-7* and *atp2-12* alleles in suppressing ρ° lethality, we disrupted the *ATP*δ (26) and *ATP*ε (27) genes. Inactivation of either δ or ε in strain CK401/1 (*atp1-7* γΔ) yielded CK408 (*atp1-7* γΔ δΔ) and CK409 (*atp1-7* γΔ εΔ), respectively, which were both respiration deficient (Fig. 4). More importantly, CK408 and CK409 remained EBʳ with a growth rate comparable to that of CK401/1 (*atp1-7* γΔ) on the EB plates. Likewise, disruption of either δ or ε in CK400 (*atp2-12* γΔ) yielded CK405 (*atp2-12* γΔ δΔ) and CK406 (*atp2-12* γΔ εΔ), respectively. Both CK405 and CK406 remained resistant to EB (Fig. 4).

Strains with triple disruptions were constructed in the *atp1-7* and *atp2-12* backgrounds. The *ATP3*, *ATP*δ, and *ATP*ε genes were successively inactivated in CK392/7 and CK391/18 to generate CK412/1 (*atp1-7* γΔ δΔ εΔ) and CK410/6 (*atp2-12* γΔ δΔ εΔ), respectively. When examined on EB medium, we found that both CK412/1 and CK410/6 are resistant to EB (Fig. 4). The results
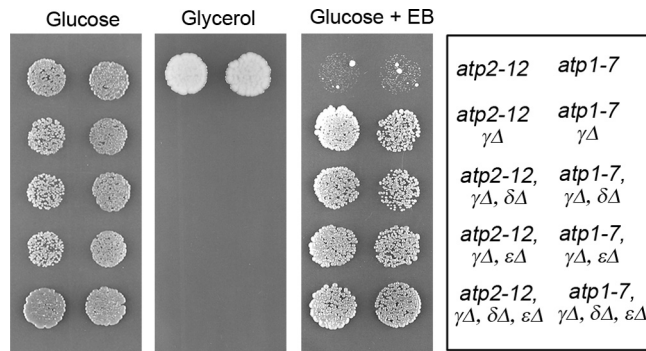
FIG 4 The δ and ε subunits are not required for the suppressor phenotype of the mutant γ-less F$_1$-ATPase. The *K. lactis* strains were grown in YPD medium overnight, diluted in water, and spotted on YPD (glucose), YPG (glycerol), and EB media. Cells were grown for 5 days at 28°C before being photographed. The strains used are identified by their genotypes in the template on the right and consist of strains CK392/7 (*atp1-7*), CK401 (*atp1-7 γΔ*) CK408 (*atp1-7 γΔ δΔ*), CK409 (*atp1-7 γΔ εΔ*), CK412/1 (*atp1-7 γΔ δΔ εΔ*), CK391/18 (*atp2-12*), CK400 (*atp2-12 γΔ*), CK405 (*atp2-12 γΔ δΔ*), CK406 (*atp2-12 γΔ εΔ*), and CK410/6 (*atp2-12 γΔ δΔ εΔ*).

indicate that γ, δ, and ε are all dispensable for the suppressor phenotype of the *atp1-7* and *atp2-12* alleles.

The *atp1-7* and *atp2-12* alleles enhance ATP hydrolysis in the γ-less F$_1$ subcomplex. We speculated that the *atp1-7* and *atp2-12* mutations in the α and β subunits may increase the ATP hydrolysis activity of the F$_1$ subcomplex lacking γ. The γ-independent ATPase activity may be too low with the wild-type α and β to suppress ρ° lethality. To test this idea, we measured the ATPase activity of isolated mitochondria in the absence and presence of oligomycin. As shown in Table 2, the γ-less strain CK306 expressing the wild-type α and β subunits retained only 5.1% of the native F$_1$-dependent ATPase activity. The activity was increased to 21.7% and 44.6% in strains CK308 (*atp1-7 γΔ*) and CK307 (*atp2-12 γΔ*), respectively. These activities are oligomycin insensitive, as expected, because the γ-less complex would not be physically coupled to F$_o$, where oligomycin binds.

We found that the *atp1-7 atp2-12* double mutant CK314-2B had only 10.8% of the wild-type ATPase activity. It was also respiration deficient on YPG medium in the presence of γ (Fig. 2). The two mutations were apparently incompatible for both hydro-

lysis and synthesis of ATP, although the single mutants retained partial respiratory growth. The disruption of *ATP3* in the double mutant (CK326) slightly increased ATPase activity. This rather subtle change is apparently sufficient for keeping ρ° cells viable. Interestingly, the *atp1-7* and *atp2-12* single mutants had oligomycin-sensitive ATPase activity higher than that of the wild type in the presence of the γ subunit, despite the fact that they were unable to maintain cell viability under ρ° conditions. It is apparent that the γ subunit stimulates ATP hydrolysis under ρ$^+$ conditions but inhibits the suppressor activity of the *atp1-7* and *atp2-12* mutants under ρ° conditions.

The γ-less subcomplexes are structurally labile *in vitro*. We attempted to purify the mutant γ-less subcomplexes so that their biochemical properties could be further characterized. A His$_6$ tag was introduced at the C terminus of the wild-type *ATP1* and the mutant *atp1-12* alleles. These alleles were integrated into the *leu2* locus of CK333 (αΔ γΔ). The untagged *ATP1* was also chromosomally integrated as a control. As expected, all the strains remained respiration deficient because of the loss of γ (Fig. 5A). The reintroduction of the His$_6$-tagged *atp1-7*, but not the His$_6$-tagged wild-type *ATP1*, conferred a robust growth phenotype on EB medium. The strong suppressor phenotype was therefore caused by the *atp1-7* allele and not the His$_6$ tag.

Isolated mitochondria were sonicated to release the His$_6$-tagged γ-less F$_1$ subcomplexes, which were purified by nickel column chromatography. We found that Atp1-His$_6$ and Atp1^{F446I}-His$_6$ were successfully pulled down together with the β subunit (Fig. 5B). This suggests that the α subunit is associated with β and likely to form a subcomplex *in vivo* to hydrolyze ATP in the absence of γ. We found that in the pull-down products, the stoichiometry between α and β varied substantially in different experiments. It is likely that the subcomplexes are unstable *in vitro* (see below) and that the unassembled α and β subunits may have precipitated out at different rates during the course of the pull-down procedure. We also introduced the His$_6$-tagged *atp2-12* allele in a βΔ γΔ double mutant and attempted to pull down the α subunit. Atp2^{G419D}-His$_6$ was poorly recovered by nickel column chromatography, suggesting that the C terminus of the β subunit is not as accessible as that of the α protein.

Surprisingly, we could not detect significant ATP-hydrolyzing activity with the pull-down products from either *ATP1* or *atp1-7*

TABLE 2 ATP hydrolysis activity of γ-less F$_1$-ATPases

| Strain | Genotype | Growth on EB | ATPase activity (μmol ATP hydrolyzed/min/mg protein)[a] | | F$_1$-d[b] | F$_1$-d/wild type (%) |
			Without oligomycin	With oligomycin		
PM6-7A	Wild type	−	1.78 ± 0.10	0.42 ± 0.10	1.57	100
CK196/1	*atp1Δ αΔ*	−	0.21 ± 0.0	0.21 ± 0.01	0	0
CK306	*γΔ*	−	0.29 ± 0.01	0.22 ± 0.01	0.08	5.1
CW15-6C	*atp1-7*	−	2.13 ± 0.04	0.56 ± 0.01	1.92	122.3
CK308	*atp1-7 γΔ*	+	0.55 ± 0.07	0.46 ± 0.01	0.34	21.7
CW14-4D	*atp2-12*	−	3.75 ± 0.09	0.56 ± 0.04	3.54	225.5
CK307	*atp2-12 γΔ*	+	0.91 ± 0.12	0.87 ± 0.16	0.7	44.6
CK314-2B	*atp2-12 atp1-7*	−	0.38 ± 0.0	0.31 ± 0.01	0.17	10.8
CK326	*atp2-12 atp1-7 γΔ*	+	0.44 ± 0.03	0.29 ± 0.01	0.23	14.6

[a] The values are averages ± standard deviations of three independent experiments.

[b] F$_1$-dependent ATPase activity, deduced from the total ATPase activity subtracted from the non-F$_1$-ATPase activity of CK196/1, expressed as μmol ATP hydrolyzed/min/mg protein.
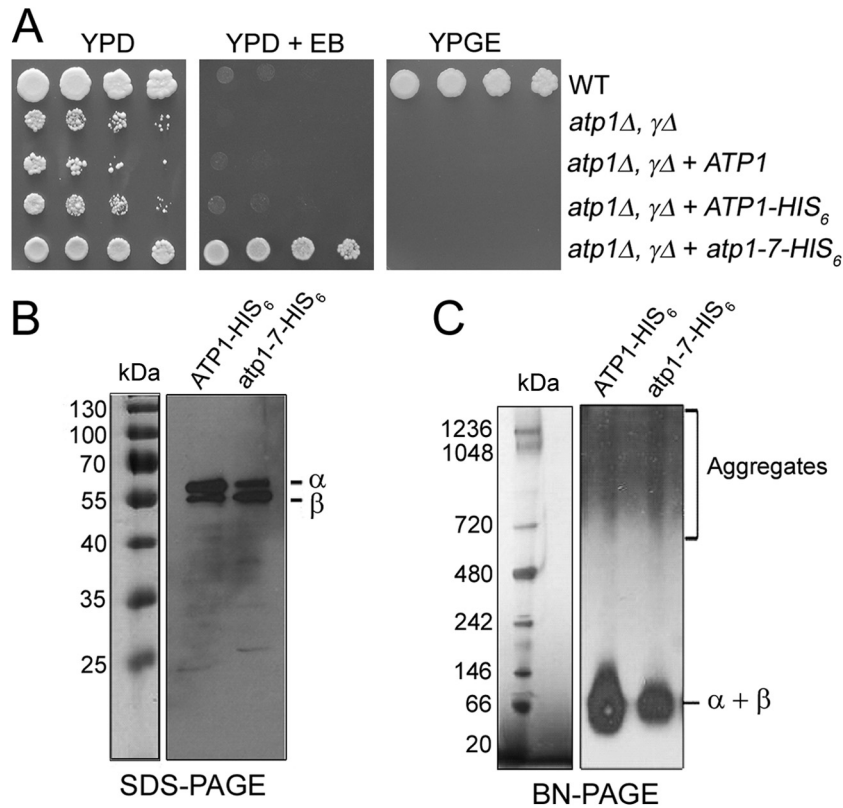
FIG 5 Purification and characterization of γ-less F$_1$-ATPases. (A) The chromosomal integration of *atp1-7*-His$_6$, but not *ATP1*-His$_6$ or *ATP1*, into *atp1*Δ γΔ cells suppresses the ρ^o lethal phenotype on YPD medium supplemented with EB. (B) Western blot analysis showing the copurification of Atp1-7-His$_6$ and Atp1-HiS$_6$ with the β subunit after nickel column chromatography. (C) BN-PAGE analysis of purified αF446I-His$_6$/β and α-His$_6$/β complexes. The protein samples were resuspended in Coomassie G-250 to a final concentration of 0.5% before electrophoresis. The proteins were visualized by immunoblotting using antibodies against the α and β subunits of F$_1$-ATPase.

cells. This suggests that the γ-less subcomplex may be structurally and functionally labile *in vitro*. By applying the pull-down products to BN-PAGE, we found that the α and β subunits were present either in a monomeric form or in a wide range of molecular species of >720 kDa, which is indicative of aggregate formation (Fig. 5C). No band of ~300 kDa suggestive of an α$_3$β$_3$ complex was visible.
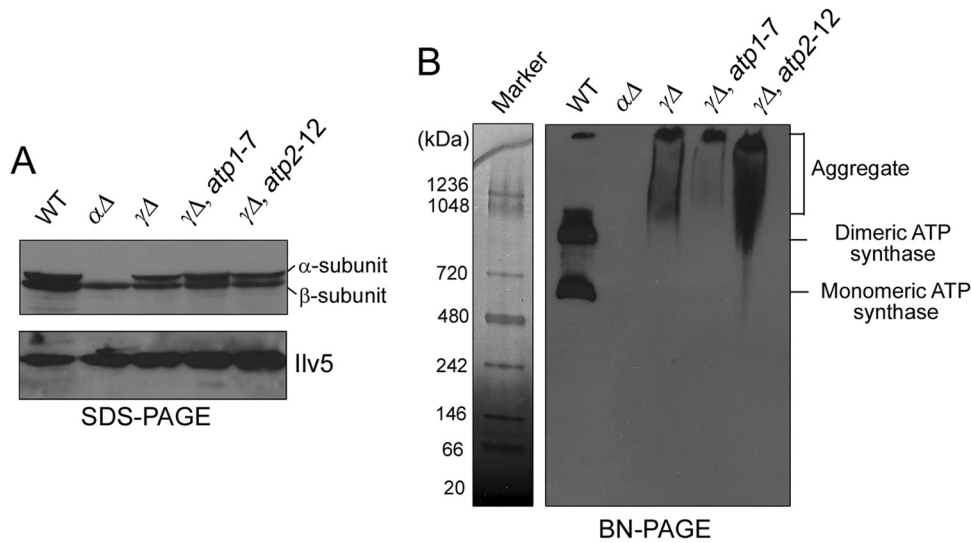
Western blot analysis of mitochondrial lysates showed that the α and β subunits were not degraded in the absence of the γ subunit (Fig. 6A). To exclude the possibility that the *in vitro* instability of the γ-less F$_1$-ATPase described above was not an artifact of the harsh conditions applied during the pull-down procedure and was not caused by His$_6$ tagging, we directly analyzed digitonin-solubilized mitochondria from untagged strains by BN-PAGE. As shown in Fig. 6B, the wild-type ATP synthase was resolved in both the monomeric and dimeric forms. In the γ-less strains, regardless of the presence or absence of a suppressor mutation, the untagged α and β subunits were detected in a wide zone of high molecular mass, indicative of protein aggregation. Thus, the γ-less F$_1$ immediately released from mitochondria is as unstable as that in the pull-down samples. These observations confirm that the γ-less F$_1$ complexes, which putatively hydrolyze ATP in mitochondria, are labile *in vitro* under the gel electrophoresis conditions.

We finally examined the assembly state of the γ-less F$_1$ complexes by directly applying the pull-down products on a size exclusion column. The resulting fractions were analyzed by Western blot analysis (Fig. 7A and B). Indeed, we found that the F$_1$ subunits did not form the distinct peak of ~300 kDa expected for an α$_3$/β$_3$ complex. Instead, they were distributed in fractions with molecular masses corresponding to species ranging from monomers to large aggregates. No significant difference in the assembly state was found with or without the presence of the *atp1-7* allele in the γ-less complexes. We also observed that the size variation of the γ-less F$_1$ deduced from size exclusion chromatography was apparently greater than that from the BN-PAGE experiment (Fig. 6B). In the latter case, molecular species of <720 kDa were barely visible. These proteins may be sensitive to electrophoresis and form molecular species that do not enter the gel. Overall, the data showed that the αβ subcomplexes are very labile and can be readily dissociated and aggregated. This property may account for the loss of ATPase activity *in vitro*.

DISCUSSION

The F$_1$-ATPase is an extremely robust molecular machine. ATP hydrolysis by the three catalytic β subunits drives the rotation of the central γ rotor at a speed of as high as 10,000 rounds per minute (28). This unusual capacity is achieved by a high degree of cooperativity between the three catalytic sites that undergo sequential conformational changes. It has long been believed that the central γ rotor plays a key role in mediating cooperative ATP hydrolysis (29). The γ subunit is situated within the α$_3$β$_3$ ring and is proposed to determine the conformational and catalytic states

FIG 6 Analysis of the γ-less F$_1$ complexes from isolated mitochondria. (A) Western blot analysis showing the steady-state levels of the α and β subunits in isolated mitochondria from the wild-type (PM6-7A), αΔ (CK196/1), γΔ (CK204), γΔ atp1-7 (CK308), and γΔ atp2-12 (CK307) strains. The mitochondrial matrix protein Ilv5 was used as a sample loading control. (B) BN-PAGE analysis of digitonin-solubilized mitochondria showing the aggregation of the γ-less F$_1$ complexes, which were visualized by immunoblotting using antibodies against the α and β subunits.
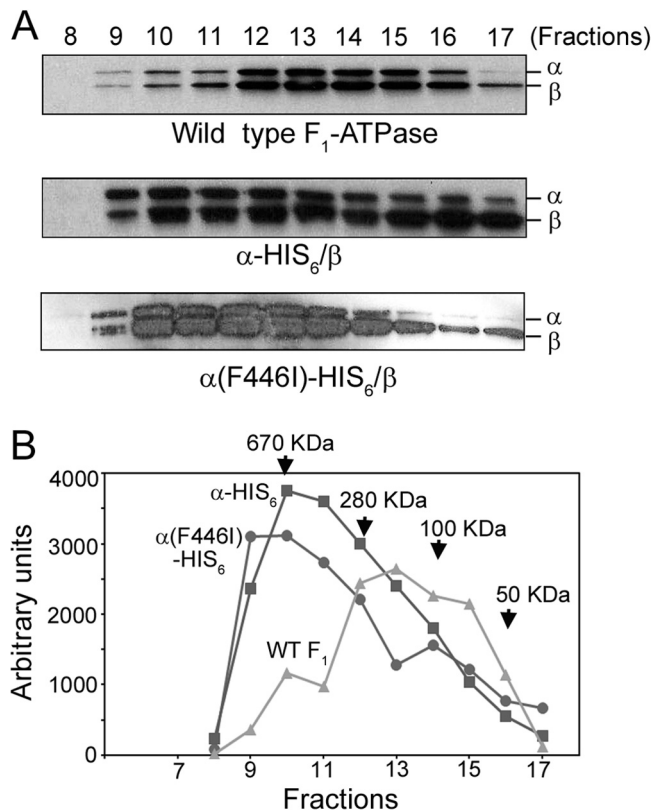
FIG 7 Analysis of γ-less F$_1$-ATPases by size exclusion chromatography. The α-His$_6$ and αF446I-His$_6$ pull-down products were analyzed on a calibrated S200 column. (A) Western blot analysis showing the elution profile of F$_1$ subunits. The wild-type F$_1$-ATPase was purified by chloroform extraction of submitochondrial particles and was used as a control. (B) Relative distribution of the F$_1$ α subunit in the fractions from size exclusion chromatography.

of β subunits during the catalytic cycle. ATP binding and hydrolysis by one catalytic β subunit drive the unidirectional rotation of the rotor γ subunit through β-γ interactions. The rotating γ in turn induces conformational changes in the next β subunit to enhance its catalytic activity. However, accumulating evidence has emerged to support the idea that the α$_3$β$_3$ subcomplex can intrinsically catalyze cooperative ATP hydrolysis independently of γ. Early studies have shown an assembled and catalytically active γ-less complex in the thermophilic bacterium PS3 F$_1$-ATPase (30, 31). Genetic studies also supported the assembly of an active F$_1$ lacking γ in S. cerevisiae mitochondria (32). The mitochondrial γ-less F$_1$ has an undetectable ATPase activity (25), whereas the isolated PS3 α$_3$β$_3$ subcomplex showed 20 to 25% of the ATPase activity of the α$_3$β$_3$γ complex. Although the PS3 α$_3$β$_3$ subcomplex is easily dissociated when the enzyme is diluted, incubated at high and low temperatures, and subjected to native polyacrylamide gel electrophoresis, it appears to exhibit similar cooperative kinetics as α$_3$β$_3$γ. The data support the idea that kinetic cooperativity is an intrinsic property of the α$_3$β$_3$ core (31) and that γ is critical for structural stabilization rather than an essential component for cooperativity. In contrast, a subsequent study reported very limited cooperativity by the α$_3$β$_3$ subcomplex (33).

More recently, the Noji group of researchers used high-speed atomic force microscopy and observed ATP-induced dynamic conformational changes in the β subunits of an α$_3$β$_3$ complex from the thermophilic bacterium PS3 (34, 35). At a given time, only one β subunit assumes the open state for ATP binding. When changed to the closed state, the neighboring β subunit is converted to the open state. A unidirectional propagation of the open state was elegantly documented. These observations provide direct evidence for a cooperative catalytic mechanism within the α$_3$β$_3$ core. The γ central stalk is, no doubt, very important for the assembly of ATP synthase and for coupling proton-driven rotation in F$_o$ to conformational changes in β during ATP synthesis, but it is not absolutely required for catalytic cooperativity during ATP hydrolysis by α$_3$β$_3$. This is consistent with an early observa-

tion that the association of α with a nucleotide-bound β subunit induces asymmetry in F$_1$ lacking the central γ rotor (36).

In the present report, we show that the γ-less F$_1$-ATPase from *K. lactis* has a barely detectable ATPase activity in isolated mitochondria, like the γ-less mutant of *S. cerevisiae* (25). This activity is enhanced by the αF446I and βG419D mutations, where the mutant γ-less F$_1$ complexes retain 21.7 and 44.6% of the wild-type γ-containing F$_1$ activity, respectively. The mutation-induced recovery of the ATPase activity can be phenotypically scored by the maintenance of cell viability in *K. lactis* under ρ^o conditions. The dramatically increased ATP hydrolysis activity supports the presence of a robust cooperativity between the catalytic sites independently of the central γ rotor, as a unisite catalytic mode would be expected to have an activity 10^5- to 10^6-fold lower than that of a cooperative mechanism (37, 38). We have not been able to determine the catalytic kinetics of the γ-less enzymes with or without the presence of suppressor mutations. These subcomplexes seem to be extremely labile. They form complexes of various sizes and are readily dissociated and aggregated *in vitro*, as revealed by BN-PAGE and size exclusion chromatography. The γ-less subcomplexes would be expected to be at least partially assembled *in vivo* to hydrolyze ATP, which allows the survival of ρ^o cells. It is possible that the protein-dense environment and/or the presence of F$_1$-specific chaperones (e.g., Atp11, Atp12, and Fmc1) (39–44) in the mitochondrial matrix may stabilize the γ-less subcomplexes *in vivo*.

Several explanations for the stimulation of ATP hydrolysis by the αF446I and βG419D mutations in the γ-less mitochondrial F$_1$-ATPases may be offered. First, as αPhe446 and βGly419 are located on the α-β interface, it is possible that the mutations structurally stabilize the γ-less complexes. However, on the basis of currently available data, this is unlikely to be the case. We found that Atp1-His$_6$ can pull down the β subunit as efficiently as Atp1^{F446I}-His$_6$. In other words, wild-type α and β subunits are likely to be as efficient as their mutant counterparts at interaction with their assembly partners *in vivo*, but it might be expected that in both cases the resulting complexes would be more unstable than native F$_1$. Furthermore, size exclusion chromatography confirmed that the γ-less F$_1$ forms molecular species of various sizes, regardless of the presence or absence of the αF446I mutation.

Alternatively, it can be speculated that the αF446I and βG419D mutations in the *K. lactis* F$_1$-ATPase stimulate ATP hydrolysis activity by altering the α-β interactions, with this alteration increasing the cooperativity within the α$_3$β$_3$ subcomplex. The mechanisms of γ-independent ATP hydrolysis and catalytic cooperativity are currently unclear (45). Gly419 in the yeast F$_1$ is located on the N-terminal edge of the DELSEED loop in the β subunit and Phe446 is located on the N-terminal edge of an equivalent loop in the α subunit (46) (Fig. 3A). These loops connect two long α helices and have previously been proposed to mediate torque transmission through interactions with γ. They are rich in negatively charged residues that may interact with the positive surface, known as the "ionic track," on the γ subunit (47). However, several studies have shown that the DELSEED loop may not be critical for torque transmission and rotational catalysis. Replacement of the acidic residues in the DELSEED loop by alanine has little effect on the rotary torque (48). The *Bacillus* PS3 F$_1$-ATPase with deletions in the DELSEED loop retains ATP hydrolysis activity through a rotational mechanism (49). The bacterial enzyme with the disruption of all predicted interactions be-

tween the DELSEED loop and γ by mutagenesis can still catalyze unidirectional rotation (50). Thus, specific interactions between the DELSEED loop and γ are not essential for cooperativity and the kinetic power of F$_1$-ATPase.

We speculate that in *K. lactis*, the αF446I and βG419D mutations may alter the α-β interactions, thereby improving catalytic cooperativity in the γ-less conformation. Although a structure of the yeast α$_3$β$_3$ ring is currently unavailable, it would seem reasonable to predict that the N-terminal edge of the DELSEED loops in the α and β subunits, where Phe446 and Gly419, respectively, are located, may alter interactions with the adjacent β and α subunits. The Yoshida group has previously solved the α$_3$β$_3$ subcomplex of the thermophilic *Bacillus* PS3 F$_1$-ATPase (51). In the absence of γ, the nucleotide-free α$_3$β$_3$ subcomplex exists in a perfect 3-fold symmetry. The αPhe398 residue, equivalent to αPhe446 in *K. lactis* at the N-terminal edge of the DELSEED loop, is on the interface with the N-terminal α helix of the DELSEED loop in the adjacent β subunit, with an estimated distance of less than 6 Å (Fig. 3B and C). It is possible that in the *K. lactis* γ-less enzyme, the replacement of αPhe446 with isoleucine alters the interactions with the N-terminal α helix on the β subunit, which changes catalytic kinetics or cooperativity. Likewise, replacement of βGly419 (or βGly388 in *Bacillus* F$_1$) with aspartic acid at the N-terminal edge of the DELSSED loop may alter the length and properties of the N-terminal α helix of the DELSEED loop in the β subunit. This may change the interactions with the C-terminal edge of the DELSEED loop on the adjacent α subunit. Because the DELSEED loops are expected to be structurally flexible, it is currently difficult to predict how the mutations exactly affect the α-β interactions during ATP hydrolysis in the γ-less subcomplexes.

The suppression of ρ^o lethality by the αF446I and βG419D mutations is much more effective in the γ-less configurations. We showed that the presence of γ inhibits the *in vivo* suppressor activity of the mutant alleles (Fig. 1A). The occupancy of the central cavity by γ appears to mask the prosurvival effects of the suppressor mutations. Consistent with its low ATP hydrolysis activity, the wild-type *K. lactis* α$_3$β$_3$ subcomplex is unable to suppress ρ^o lethality. It is possible that the γ subunit acts as a mediator for stimulating α-β interactions during cooperative catalysis by the native F$_1$-ATPase. The αF446I and βG419D mutations may bypass the requirement for γ by directly stimulating α-β interactions.

It remains mysterious with regard to the wild-type α$_3$β$_3$γ complex, which is active in ATP hydrolysis but is unable to suppress ρ^o lethality *in vivo*. As previously suggested, the wild-type enzyme may have a high K_m for ATP, which would not allow hydrolysis of sufficient ATP in ρ^o cells where ATP is scarce (18). In this context, we cannot completely exclude the possibility that in the γ-less configuration the αF446I and βG419D mutations promote cell survival by lowering the K_m for ATP, which increases ATP turnover and therefore the membrane potential in ρ^o cells by a mechanism independent of the ATP synthase complex. The γ-less *K. lactis* F$_1$-ATPase is highly unstable *in vitro*. For future studies, detailed kinetic properties of the γ-less enzymes may be tested by introducing similar mutations in a more stable enzyme, such as the thermophilic *Bacillus* PS3 α$_3$β$_3$ subcomplex. Alternatively, the ATP-hydrolyzing activity of the α$_3$β$_3$γ and α$_3$β$_3$ complexes may be inhibited *in vivo* under ρ^o conditions and the inhibition may be relieved by the suppressor mutations.

Smith and Thorsness have previously reported that the βG227S

mutation in *S. cerevisiae* F$_1$-ATPase suppresses the slow-growth phenotype of cells in which the *ATP3* gene encoding the γ subunit is disrupted (52). Because the *atp3* mutant is unable to maintain mtDNA, cell survival would require a robust ATP hydrolysis by F$_1$ to maintain the mitochondrial inner membrane potential through the electrogenic ATP^{-4} (cytosol)/ADP^{-3} (matrix) exchange. The γ-less F$_1$ is likely ineffective in ATP hydrolysis, but it may be increased by the βG227S mutation. Indeed, it was found that ATP hydrolysis was increased from 5.6% of that for the native F$_1$ in cells expressing the wild-type α and β to 19% of that in cells expressing the wild-type α and the βG227S allele. βGly227 is located close to the conserved arginine finger domain of the active site. The βG227S mutation may potentially increase ATP hydrolysis in the absence of the γ subunit. Interestingly, the arginine finger has previously been proposed to sense the presence (or absence) of the γ-phosphate of ATP and to contribute to the cooperativity of the stator ring in F$_1$-ATPase (53, 54).

In summary, although the exact mechanism remains to be determined, our data provide *in vivo* evidence for robust ATP-hydrolyzing activity by γ-less mitochondrial F$_1$-ATPases. This is possible only when specific mutations are introduced at the N-terminal edge of the DELSEED loop in either the α or the βsubunit. The data provide unambiguous evidence for the importance of these two sites in promoting ATP hydrolysis in a γ-independent manner. These findings are consistent with the notion that an effective α-β interaction is critical for ATP hydrolysis by the α$_3$β$_3$ ring. This mode of ATP hydrolysis is reminiscent of that of some AAA-ATPases whose catalytic activity is independent of a central rotor (45). Thus, the genetic system that we developed in *K. lactis* could be further explored in the future for effectively dissecting the mechanism of α-β interactions without the interference from the γ subunit.

REFERENCES

1. **Ephrussi B, Hottinguer H, Tavlitzki J.** 1949. Action de l'acriflavine sur les levures. II. Etude génétique du mutant "petite colonie". Ann. Inst. Pasteur (Paris) **76**:419–442.
2. **Bulder CJ.** 1964. Lethality of the petite mutation in petite negative yeasts. Antonie Van Leeuwenhoek **30**:442–454.
3. **Bulder CJ.** 1964. Induction of petite mutation and inhibition of synthesis of respiratory enzymes in various yeasts. Antonie Van Leeuwenhoek **30**:1–9.
4. **Faye G, Fukuhara H, Grandchamp C, Lazowska J, Michel F, Casey J, Getz GS, Locker J, Rabinowitz M, Bolotin-Fukuhara M, Coen D, Deutsch J, Dujon B, Netter P, Slonimski PP.** 1973. Mitochondrial nucleic acids in the petite colonie mutants: deletions and repetition of genes. Biochimie **55**:779–792.
5. **Chen XJ, Clark-Walker GD.** 2000. The petite mutation in yeasts: 50 years on. Int. Rev. Cytol. **194**:197–238.
6. **Chen XJ, Clark-Walker GD.** 1993. Mutations in *MGI* genes convert *Kluyveromyces lactis* into a petite-positive yeast. Genetics **133**:517–525.
7. **Chen XJ, Clark-Walker GD.** 1995. Specific mutations in alpha- and gamma-subunits of F$_1$-ATPase affect mitochondrial genome integrity in the petite-negative yeast *Kluyveromyces lactis*. EMBO J. **14**:3277–3286.
8. **Chen XJ, Clark-Walker GD.** 1996. The mitochondrial genome integrity gene, *MGI1*, of *Kluyveromyces lactis* encodes the beta-subunit of F$_1$-ATPase. Genetics **144**:1445–1454.
9. **Clark-Walker GD, Hansbro PM, Gibson F, Chen XJ.** 2000. Mutant residues suppressing rhoº-lethality in *Kluyveromyces lactis* occur at contact sites between subunits of F$_1$-ATPase. Biochim. Biophys. Acta **1478**:125–137.
10. **Boyer PD.** 1997. The ATP synthase—a splendid molecular machine. Annu. Rev. Biochem. **66**:717–749.
11. **Duncan TM.** 2004. The ATP synthase: parts and properties of a rotary motor, p 203–275. *In* Hackney DD, Tamanoi F (ed), The enzymes, vol XXIII. Energy coupling and molecular motors, 3rd ed. Elsevier Academic Press, New York, NY.
12. **Abrahams JP, Leslie AG, Lutter R, Walker JE.** 1994. Structure at 2.8 Å resolution of F$_1$-ATPase from bovine heart mitochondria. Nature **370**:621–628.
13. **Noji H, Yasuda R, Yoshida M, Kinosita K, Jr.** 1997. Direct observation of the rotation of F$_1$-ATPase. Nature **386**:299–302.
14. **Klingenberg M, Rottenberg H.** 1977. Relation between the gradient of the ATP/ADP ratio and the membrane potential across the mitochondrial membrane. Eur. J. Biochem. **73**:125–130.
15. **Dupont CH, Mazat JP, Guerin B.** 1985. The role of adenine nucleotide translocation in the energization of the inner membrane of mitochondria isolated from rho$^+$ and rhoº strains of *Saccharomyces cerevisiae*. Biochem. Biophys. Res. Commun. **132**:1116–1123.
16. **Kominsky DJ, Brownson MP, Updike DL, Thorsness PE.** 2002. Genetic and biochemical basis for viability of yeast lacking mitochondrial genomes. Genetics **162**:1595–1604.
17. **Weber ER, Rooks RS, Shafer KS, Chase JW, Thorsness PE.** 1995. Mutations in the mitochondrial ATP synthase gamma subunit suppress a slow-growth phenotype of *yme1* yeast lacking mitochondrial DNA. Genetics **140**:435–442.
18. **Clark-Walker GD.** 2003. Kinetic properties of F$_1$-ATPase influence the ability of yeasts to grow in anoxia or absence of mtDNA. Mitochondrion **2**:257–265.
19. **Wang Y, Singh U, Mueller DM.** 2007. Mitochondrial genome integrity mutations uncouple the yeast *Saccharomyces cerevisiae* ATP synthase. J. Biol. Chem. **282**:8228–8236.
20. **Arsenieva D, Symersky J, Wang Y, Pagadala V, Mueller DM.** 2010. Crystal structures of mutant forms of the yeast F$_1$ ATPase reveal two modes of uncoupling. J. Biol. Chem. **285**:36561–36569.
21. **Chen XJ.** 1996. Low- and high-copy-number shuttle vectors for replication in the budding yeast *Kluyveromyces lactis*. Gene **172**:131–136.
22. **Boldogh IR, Pon LA.** 2007. Purification and subfractionation of mitochondria from the yeast *Saccharomyces cerevisiae*. Methods Cell Biol. **80**:45–64.
23. **Mueller DM, Puri N, Kabaleeswaran V, Terry C, Leslie AG, Walker JE.** 2004. Ni-chelate-affinity purification and crystallization of the yeast mitochondrial F$_1$-ATPase. Protein Expr. Purif. **37**:479–485.
24. **Taussky HH, Shorr E.** 1953. A microcolorimetric method for the determination of inorganic phosphorus. J. Biol. Chem. **202**:675–685.
25. **Paul MF, Ackerman S, Yue J, Arselin G, Velours J, Tzagolof A, Ackermann S.** 1994. Cloning of the yeast *ATP3* gene coding for the gamma-subunit of F$_1$ and characterization of *atp3* mutants. J. Biol. Chem. **269**:26158–26164.
26. **Hansbro PM, Chen XJ, Clark-Walker GD.** 1998. Allele specific expression of the Mgi⁻ phenotype on disruption of the F$_1$-ATPase delta-subunit gene in *Kluyveromyces lactis*. Curr. Genet. **33**:46–51.
27. **Chen XJ.** 2000. Absence of F$_1$-ATPase activity in *Kluyveromyces lactis* lacking the epsilon subunit. Curr. Genet. **38**:1–7.
28. **Yasuda R, Noji H, Yoshida M, Kinosita K, Jr, Itoh H.** 2001. Resolution of distinct rotational substeps by submillisecond kinetic analysis of F$_1$-ATPase. Nature **410**:898–904.
29. **Wang H, Oster G.** 1998. Energy transduction in the F$_1$ motor of ATP synthase. Nature **396**:279–282.
30. **Miwa K, Yoshida M.** 1989. The alpha 3 beta 3 complex, the catalytic core of F$_1$-ATPase. Proc. Natl. Acad. Sci. U. S. A. **86**:6484–6487.
31. **Kagawa Y, Ohta S, Otawara-Hamamoto Y.** 1989. Alpha 3 beta 3 complex of thermophilic ATP synthase: catalysis without the gamma-subunit. FEBS Lett. **249**:67–69.
32. **Lai-Zhang J, Xiao Y, Mueller DM.** 1999. Epistatic interactions of deletion mutants in the genes encoding the F$_1$-ATPase in yeast *Saccharomyces cerevisiae*. EMBO J. **18**:58–64.
33. **Kaibara C, Matsui T, Hisabori T, Yoshida M.** 1996. Structural asymmetry of F$_1$-ATPase caused by the gamma subunit generates a high affinity nucleotide binding site. J. Biol. Chem. **271**:2433–2438.

34. **Uchihashi T, Iino R, Ando T, Noji H.** 2011. High-speed atomic force microscopy reveals rotary catalysis of rotorless F$_1$-ATPase. Science **333:** 755–758.

35. **Iino R, Noji H.** 2012. Rotary catalysis of the stator ring of F$_1$-ATPase. Biochim. Biophys. Acta **1817:**1732–1739.

36. **Burgard S, Harada M, Kagawa Y, Trommer WE, Vogel PD.** 2003. Association of alpha-subunits with nucleotide-modified beta-subunits induces asymmetry in the catalytic sites of the F$_1$-ATPase alpha$_3$beta$_3$-hexamer. Cell Biochem. Biophys. **39:**175–181.

37. **Cross RL, Grubmeyer C, Penefsky HS.** 1982. Mechanism of ATP hydrolysis by beef heart mitochondrial ATPase. Rate enhancements resulting from cooperative interactions between multiple catalytic sites. J. Biol. Chem. **257:**12101–12105.

38. **Noumi T, Taniai M, Kanazawa H, Futai M.** 1986. Replacement of arginine 246 by histidine in the beta subunit of *Escherichia coli* H$^+$-ATPase resulted in loss of multi-site ATPase activity. J. Biol. Chem. **261:**9196–9201.

39. **Ackerman SH.** 2002. Atp11p and Atp12p are chaperones for F$_1$-ATPase biogenesis in mitochondria. Biochim. Biophys. Acta **1555:**101–105.

40. **Ackerman SH, Tzagoloff A.** 1990. Identification of 2 nuclear genes (Atp11, Atp12) required for assembly of the yeast F$_1$-ATPase. Proc. Natl. Acad. Sci. U. S. A. **87:**4986–4990.

41. **Wang ZG, Ackerman SH.** 2000. The assembly factor Atp11p binds to the beta-subunit of the mitochondrial F$_1$-ATPase. J. Biol. Chem. **275:**5767–5772.

42. **Wang ZG, Sheluho D, Gatti DL, Ackerman SH.** 2000. The alpha-subunit of the mitochondrial F$_1$ ATPase interacts directly with the assembly factor Atp12p. EMBO J. **19:**1486–1493.

43. **Lefebvre-Legendre L, Salin B, Schaeffer J, Brethes D, Dautant A, Ackerman SH, di Rago JP.** 2005. Failure to assemble the alpha 3 beta 3 subcomplex of the ATP synthase leads to accumulation of the alpha and beta subunits within inclusion bodies and the loss of mitochondrial cristae in *Saccharomyces cerevisiae*. J. Biol. Chem. **280:**18386–18392.

44. **Lefebvre-Legendre L, Vaillier J, Benabdelhak H, Velours J, Slonimski PP, di Rago JP.** 2001. Identification of a nuclear gene (*FMC1*) required for

the assembly/stability of yeast mitochondrial F$_1$-ATPase in heat stress conditions. J. Biol. Chem. **276:**6789–6796.

45. **Iino R, Noji H.** 2013. Intersubunit coordination and cooperativity in ring-shaped NTPases. Curr. Opin. Struct. Biol. **23:**229–234.

46. **Kabaleeswaran V, Puri N, Walker JE, Leslie AG, Mueller DM.** 2006. Novel features of the rotary catalytic mechanism revealed in the structure of yeast F$_1$ ATPase. EMBO J. **25:**5433–5442.

47. **Ma J, Flynn TC, Cui Q, Leslie AG, Walker JE, Karplus M.** 2002. A dynamic analysis of the rotation mechanism for conformational change in F$_1$-ATPase. Structure **10:**921–931.

48. **Hara KY, Noji H, Bald D, Yasuda R, Kinosita K, Jr, Yoshida M.** 2000. The role of the DELSEED motif of the beta subunit in rotation of F$_1$-ATPase. J. Biol. Chem. **275:**14260–14263.

49. **Mnatsakanyan N, Krishnakumar AM, Suzuki T, Weber J.** 2009. The role of the betaDELSEED-loop of ATP synthase. J. Biol. Chem. **284:**11336–11345.

50. **Tanigawara M, Tabata KV, Ito Y, Ito J, Watanabe R, Ueno H, Ikeguchi M, Noji H.** 2012. Role of the DELSEED loop in torque transmission of F$_1$-ATPase. Biophys. J. **103:**970–978.

51. **Shirakihara Y, Leslie AG, Abrahams JP, Walker JE, Ueda T, Sekimoto Y, Kambara M, Saika K, Kagawa Y, Yoshida M.** 1997. The crystal structure of the nucleotide-free alpha 3 beta 3 subcomplex of F$_1$-ATPase from the thermophilic Bacillus PS3 is a symmetric trimer. Structure **5:**825–836.

52. **Smith CP, Thorsness PE.** 2005. Formation of an energized inner membrane in mitochondria with a gamma-deficient F$_1$-ATPase. Eukaryot. Cell **4:**2078–2086.

53. **Nadanaciva S, Weber J, Wilke-Mounts S, Senior AE.** 1999. Importance of F$_1$-ATPase residue alpha-Arg-376 for catalytic transition state stabilization. Biochemistry **38:**15493–15499.

54. **Kagawa R, Montgomery MG, Braig K, Leslie AG, Walker JE.** 2004. The structure of bovine F$_1$-ATPase inhibited by ADP and beryllium fluoride. EMBO J. **23:**2734–2744.

55. **Chen XJ, Wesolowski-Louvel M, Fukuhara H.** 1992. Glucose transport in the yeast *Kluyveromyces lactis*. II. Transcriptional regulation of the glucose transporter gene *RAG1*. Mol. Gen. Genet. **233:**97–105.